Electronic Supplementary Information (ESI) for

Unveiling the Potential of a Covalent Triazine Framework based on [1]benzothieno[3,2-b][1]benzothiophene (DPhBTBT-CTF) as Metal-free Heterogeneous Photocatalyst

M. Carmen Borrallo-Aniceto[a], Mercedes Pintado-Sierra[b], Antonio Valverde-González[a], Urbano Díaz[c], Félix Sánchez[b], Eva M. Maya[a] and Marta Iglesias[a]

[a] Instituto de Ciencia de Materiales de Madrid (ICMM-CSIC), Sor Juana Inés de la Cruz, 3, Cantoblanco. Madrid 28049, Spain E-mail: marta.iglesias@icmm.csic.es

[b] Instituto de Química Orgánica General (IQOG-CSIC), C/ Juan de la Cierva 3, Madrid 28006, Spain.

[c] Instituto de Tecnología Química, Universitat Politècnica de València, Consejo Superior de Investigaciones Científicas, Avenida de los Naranjos s/n, E-46022 Valencia, Spain

Table of contents

1. Materials and Characterization Methods

All of the reagents were obtained from commercial sources and used without further purification unless otherwise indicated. Solvents were dried by standard methods or by elution using a PureSolv Innovative Technology drying system.

The **microwaves** oven used were Discover SP® from CEM Corporation 3100 and/or Monowave 300 from Anton PAAR.

Elemental analysis (%C, %N %H and %S) were determined in a LECO CHNS-932 analyzer.

The **HR-MS** analysis was carried out by using an Agilent 1200 Series LC system coupled to a 6520 quadrupole-time of flight (QTOF) mass spectrometer. Acetonitrile: water (75:25, v:v) was used as mobile phase at 0.2 mL min^{-1}. The ionization source was an ESI interface working in the positive-ion mode.

Nuclear magnetic resonance **(NMR)** spectra of molecular samples were recorded with a BRUKER AVANCE III HD (Larmor frequencies of 400, 101 MHz for ^{1}H, ^{13}C) for liquids and a Bruker AV400 WB spectrometer (Larmor frequencies of 400 and 100 MHz) using 4 mm MAS probes spinning at 10 kHz rate for ^{13}C solid-state MAS-NMR measurements. The ^{13}C CP-MAS spectra were obtained using 3.5 ms contact time and 4 s relaxation time. The number of scans was 1024 of ^{13}C CP-MAS spectra.

ATR spectra were recorded on an appliance type Perkin Elmer Spectrum Two with a Fourier Transformer.

Nitrogen adsorption/desorption isotherms were measured at 77 K using a Quantachrome surface and porosity analyzer. Prior to measurement, the samples were degassed for 12 h at 100°C. Specific surface areas were determined by N_2 adsorption-desorption at 77K and the pore distribution by DFT methods. Surface area was determined by the Brunauer–Emmett–Teller (BET) method. The **CO$_2$ gas adsorption** measurements were carried out using a Micromeritics ASAP 2010 instrument. The samples were degassed at 150ºC in high vacuum before measurements. The surface areas and pore volumes were determined via CO_2 adsorption at 273 K by the Dubinin-Astakhov method.

Thermogravimetric and differential thermal analyses (**TGA**) were conducted with a TA Instruments Model TA-Q500 analyzer. The samples were heated from 40 to 800 ºC under air atmosphere with a heating rate 10 ºC/min.

EPR spectra were recorded at 100k on a Bruker EMX-12 instrument operating in X band at 9.5GHz, modulation amplitude of 1G and modulation frequency of 100KHz.

The morphology was analyzed by a Field Emission Scanning Electron Microscopy **SEM** model Hitachi S-8000 equipped with an Energy Dispersive X-ray spectroscopy (EDAX) analyzer, EDAX SUTW equipment (Super Ultra-Thin Window). Transmission electron microscopy **(TEM)** was performed in a JEOL model JEM-1400Flash with a STEM detector. For the analysis, a small amount

of the sample was dispersed in dichloromethane. Then, a drop was placed on a nickel grid and dried under a lamp for 2 h.

The C1s, N1s, and survey spectra were recorded using a Thermo Scientific K-Alpha instrument. Monochromatic X-ray source Al Kα (1486.6 eV) was used for all samples and experiments. The X-Ray Monochromatic spot is 400 μm in diameter. Residual vacuum in the analysis chamber was maintained at around $6x10^{-10}$ mbar. We have also employed an electron flood gun to minimize surface charging (Charge compensation). The atomic concentrations were determined from the XPS peak areas using the Shirley background subtraction technique and the Scofield sensitivity factors. The powder samples were fixed to the holder using a copper adhesive tape to ensure the powders are firmly attached during analysis.

Acquisition of chromatograms (**GC**) was done using a KONIK HRGC 4000B; with a KAP-120212 capillary column (30 m, 0.25 mm, 0.25 μm).

Fluorescence spectra were logged on a Varian Cary Eclipse fluorescence spectrophotometer equipped with 1x1 cm quartz cuvette. The width of the excitation slit and the emission slit were set to 5.0 nm.

Electrochemical measurements were carried out by using an Autolab PGSTAT302 workstation interfaced with a computer and a VMP-3e Multichannel Potentiostat.

EIS measurements. Potentiostatic electronic impedance spectra (PEIS) were collected in acetonitrile containing 0.1 M tetrabutylammonium hexafluorophosphate (NBu_4PF_6) using the same three-electrode system employed to record CVs on a Biologic Multichannel potentiostate VMP-3e with EIS capability. Experiments were collected at different bias potentials (0-2.2 V vs Ag/AgCl over a frequency range from 106 Hz to 100MHz with a signal amplitude of 10 mV.

The **photoreactor** (Figure S1) used for the reactions tested was laboratory-made and is equipped with two 30W blue LED lamps (23mW/cm²).
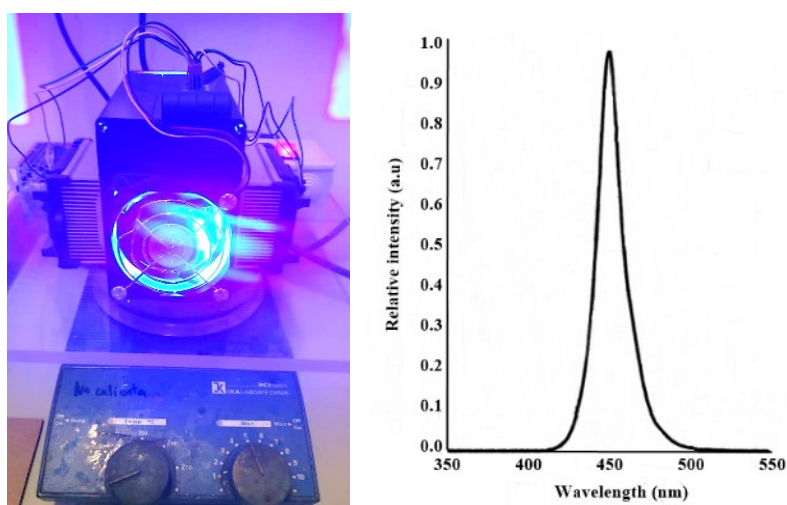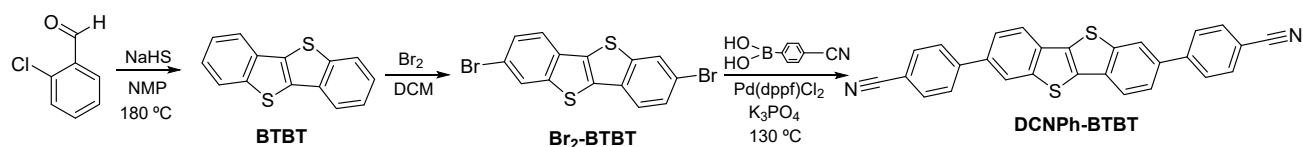

Figure S1. Photoreactor used in the reactions and light emission spectrum of the blue.

2. Synthetic procedures

2.1 Synthesis of 4,4'-(benzo[b]benzo[4,5]thieno[2,3-d]thiophene-2,7-diyl)dibenzonitrile (DCNPh-BTBT)

Scheme 1. Synthetic route to prepare DCNPh-BTBT monomer

2.1.1 Synthesis of Benzo[b]benzo[4,5]thieno[2,3-d]thiophene (BTBT)

BTBT was synthesized according to the method described in the literature.[1,2,3] **^{1}H-NMR** (400 MHz, Chloroform-d) δ (ppm): 7.8-8.0 (m, 4H), 7.4 - 7.5 (m, 4H).

2.1.2 Synthesis of 2,7-dibromobenzo[b]benzo[4,5]thieno[2,3-d]thiophene (Br$_2$-BTBT)

Br$_2$-BTBT was synthesized according to the method described in the literature.[2,3] **^{1}H-NMR** (400 MHz, Chloroform-d) δ (ppm): 8.07 (d, J = 1.8 Hz, 2H), 7.73 (d, J = 8.4 Hz, 2H), 7.58 (ddd, J = 8.4, 1.8, 0.5 Hz, 2H). **HRMS (ESI$^+$)**: m/z (M+): 397.900.

2.1.3 Synthesis of 4,4'-(benzo[b]benzo[4,5]thieno[2,3-d]thiophene-2,7-diyl)dibenzonitrile (DCNPh-BTBT)

Following a similar procedure for other BTBT-derivatives[4,5,6], in a 50 mL pressure tube, dioxane (14 mL), Br$_2$-BTBT (280 mg, 0.7mmol, 1 eq.), 4-cyanophenylboronic acid (310 mg, 2.1mmol, 3 eq.), K$_3$PO$_4$ (1.5 g, 7.0 mmol, 10 eq.), aliquat (one drop) are deaerated under argon for 30 min. Then Pd(dppf)Cl$_2$ (20 mg, 0.03mmol, 0.04 eq.) was added and the mixture bubbled with argon for additional 10 min. The tube was then closed and heated at 130°C for 48 h. The system was cooled to room temperature, the solvent removed under vacuum and water was added and the crude reaction mixture stirred for 1 h. The resultant solid was filtered and purified by recrystallization from dimethylacetamide (DMA). DCNPh-BTBT was obtained with a yield of 58% (180 mg). **^{1}H-NMR (**300 MHz, Chloroform-d) δ (ppm): 8.17 (d, J = 1.7 Hz, 1H), 8.01 (d, J = 8.3 Hz, 1H), 7.79 (d, J = 1.8 Hz, 4H), 7.72 (dd, J = 8.3, 1.7 Hz, 1H). **^{13}C-NMR** (CP-MAS solid state) δ (ppm): 143 (C-C), 138, 133, 126, 123 (Ar), 110 (CN). **HRMS (ESI$^+$)**: m/z (M$^+$): 442.0555. **FT-IR (ATR)** (cm^{-1}): 2225, 1603, 1506, 1456, 1388, 1343, 1288, 1242, 1181, 1113, 1057, 1011, 943, 842, 808, 713, 645, 569, 541, 532. **Elemental analysis** for C$_{28}$H$_{14}$N$_2$S$_2$ calcd. (found): C%, 75.9 (75.3), H%, 3.2 (3.5), N%, 6.3 (6.3), S%, 14.5 (14.3).
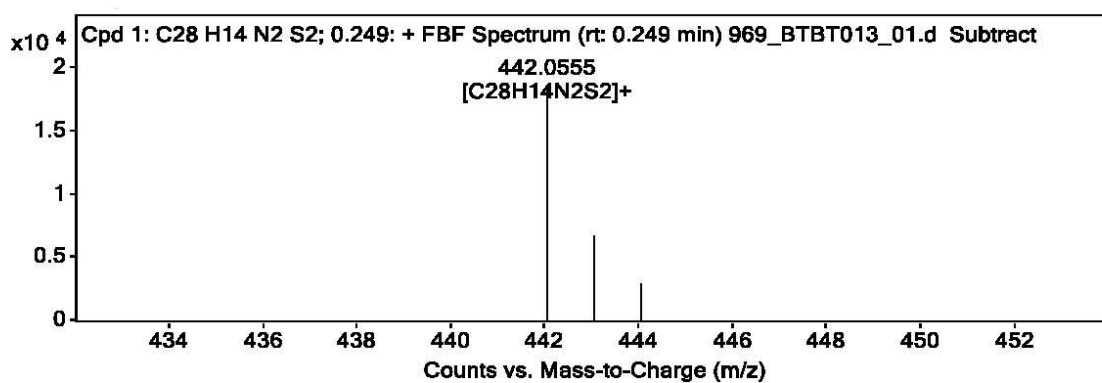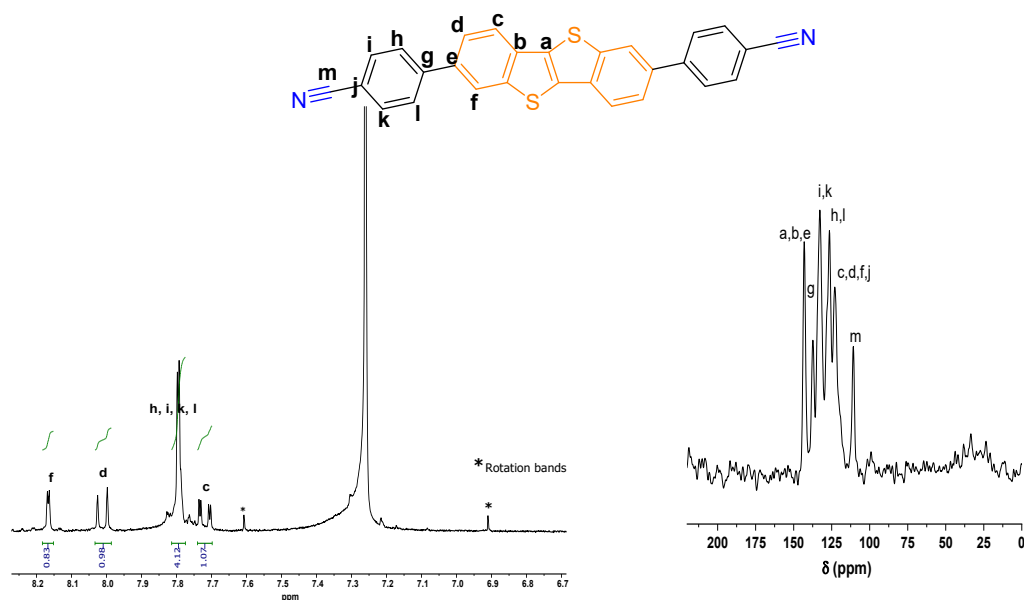
Figure S2. ^{1}H-NMR, ^{13}C-NMR and HRMS (ESI+) spectra of DCNPh-BTBT.

2.2. Synthesis of DPhBTBT-CTF

To a 10 mL MW vial fitted with a magnetic stirred, the dinitrile, DCNPh-BTBT, (100 mg, 0.22mmol, 1eq.) and trifluoromethane sulfonic acid (1 mL, 11.3mmol, 50 eq.) were added. The mixture was stirred at 200 W and 110ºC for 2h. After that, the reaction mixture is poured into an ice/water mixture (70 mL) and a water/ammonia solution (20:1) (35 mL) was added until pH 6-7. Then, the product was filtered, washed with water, ethanol and THF and dried at 100ºC under vacuum. The final brown solid was obtained in 72% yield (72 mg). **FT-IR (ATR)** (cm^{-1}): 1681.6, 1604.5, 1504.7, 1361.5, 1239.6, 1161.9, 1027, 949.13, 805.76, 755.06, 635.5. **Elemental analysis** for C$_{42}$H$_{27}$N$_3$S$_2$ calcd. (found): C%, 75.31 (69.20), H%, 4.06 (4.53), N%, 6.27 (5.60), S%, 14.36 (13.95). N/S= 0.43 (0.40)
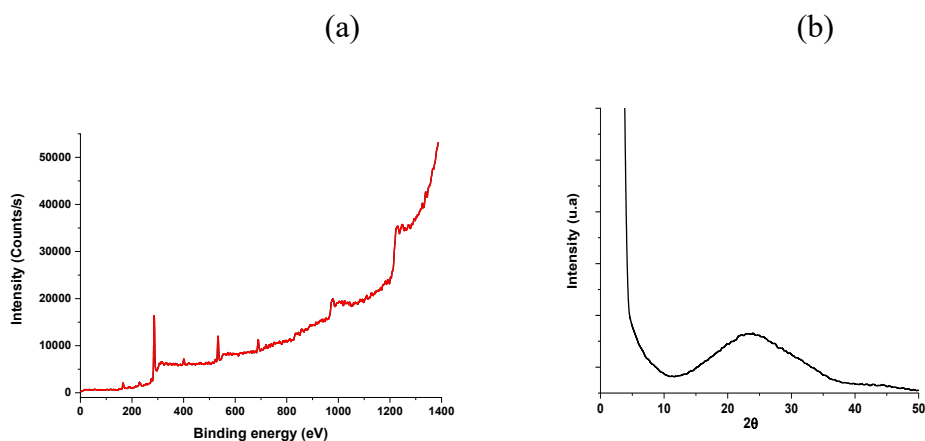
Figure S3. XPS survey spectrum (left) and Powder X-ray diffraction (right) of DPhBTBT-CTF
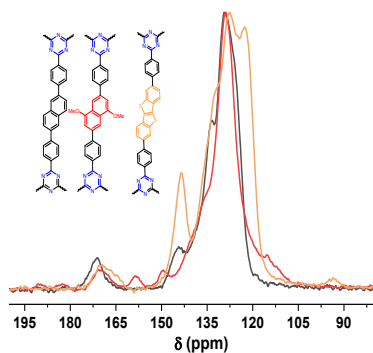
Figure S4. ^{13}C-NMR solid state spectrum of diphenyl extended-based CTFs
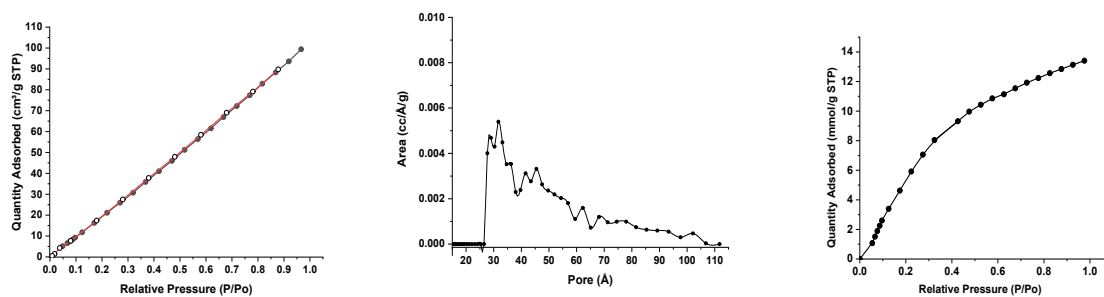
Figure S5. N$_2$ adsorption-desorption isotherms (left), pore distribution by DFT method (middle) and CO$_2$ adsorption isotherm (right) of DPhBTBT-CTF.

3. Optical characterization
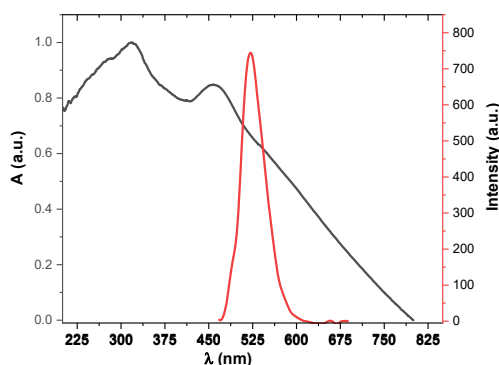
Figure S6. Optical characterization of DPhBTBT-CTF: UV-visible Absorption (black) and emission spectra (red) in acetonitrile suspension (λ_{exc} = 450 nm).

4. Electrochemical experiments

Cyclic voltammetry of DCNPh-BTBT was obtained at room temperature and 100 mV/s under nitrogen atmosphere, using a 0.1 M tetrabutylammonium hexafluorophosphate solution in CH_3CN as electrolyte. A standard three-electrode electrochemical cell was used. Potentials were referred to an Ag/AgCl (3.5M KCl) and platinum as counter electrode. The working electrode consists of a glassy carbon electrode (GCE).

Cyclic voltammetry of DPhBTBT-CTF was obtained at room temperature and 100 mV/s, under nitrogen atmosphere, using 0.1 M tetrabutylammonium hexafluorophosphate solution (CH_3CN) as electrolyte. A standard three-electrode electrochemical cell was used. Potentials were referred to an Ag/AgCl (3.5M KCl) and platinum as counter electrode. The working electrode consists of a glassy carbon electrode (GCE) coated with a homogeneous hybrid paste. The hybrid was fabricated by mixing 7 mg of high purity carbon (>99.9%) with 3 mg of the material and 80μL drop of Nafion.

Electrochemical impedance spectroscopy was obtained at 25ºC using 0.1 M tetrabutylammonium hexafluorophosphate solution (CH_3CN) as electrolyte. A standard three-electrode electrochemical cell was used. Potentials were referred to an Ag/AgCl (1 M KCl) and platinum as counter electrode. The working electrode consists of a glassy carbon electrode (GCE) coated with a homogeneous hybrid paste. The hybrid was fabricated by mixing 5 mg of the material and 1mL of a mixture of ethanol Nafion (100/1).
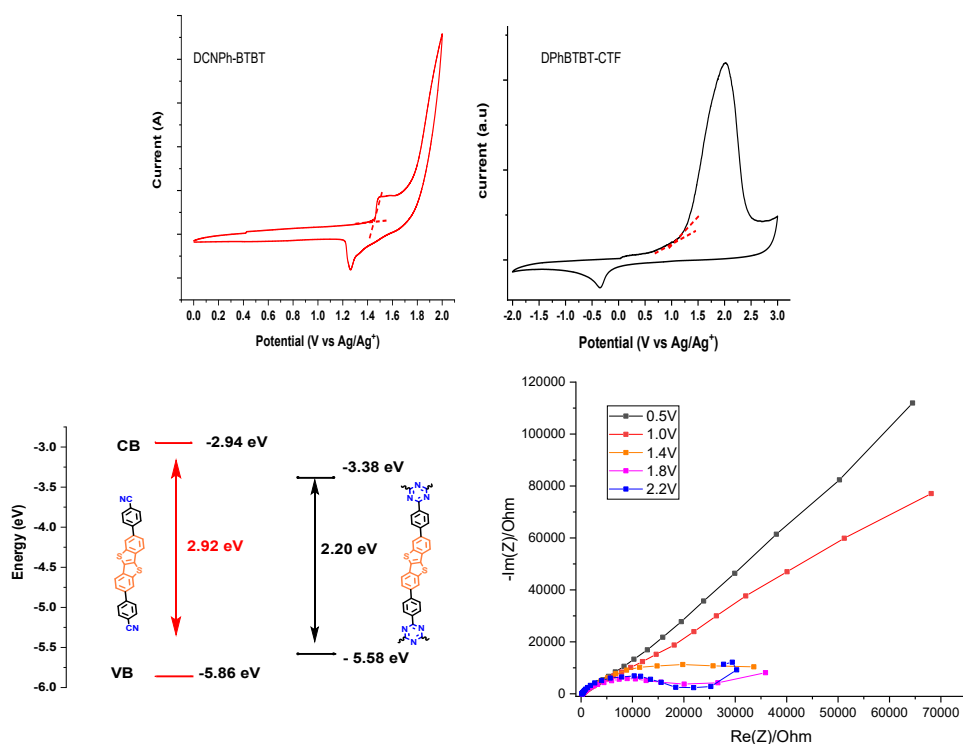
Figure S7. Top: Cyclic voltammetry. Down: HOMO and LUMO energy levels (in eV) (left) and Nyquist plots from EIS experiments (right) of DPhBTBT-CTF (from 1 MHz to 100 mHz).

Table S1. Electrochemical Properties of DPhCN-BTBT monomer and DPhBTBT-CTF.

Compound	$E_{gap}(eV)^a$	$E_{oxonset}(V)^b$	E_{HOMO} (eV)^c	E_{LUMO} (eV)^d	E_{HOMO} (V)^e	E_{LUMO} (V)^e
DCNPh-BTBT	2.92	1.46	-5.86	-2.94	1.66	-1.25
DPhBTBT-CTF	2.20	1.18	-5.58	-3.38	1.38	-0.84
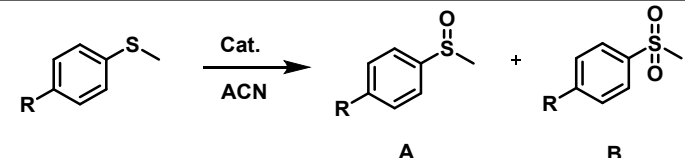
^{a}E_{gap} estimated from Tauc-Plot; ^{b}E_{ox} estimated from CV measurements vs Ag/AgCl (3.5M KCl); ^{c}E_{HOMO}= -(E_{ox} + 4.44) (eV); ^{d}E_{LUMO} = E_{HOMO} + E_{gap} ^{e}vs NHE.

5. Catalytic activity
5.1 Photoxidation reactions

General procedure: In a SUPELCO glass microreactor, the corresponding substrate (0.2 mmol), catalyst (2 mol% or 4 mol% for albendazole) and acetonitrile or tetrahydrofuran (for albendazole) (0.5 mL) are added. The suspension was purged with O_2 or air and stirred under irradiation with blue LED light (2x30W). The reactions were monitored by GC chromatography or ^{1}H-NMR.

Table S2. Control experiments for photooxidation reaction.[a]

Entry	Conditions	R	Oxidant	t (h)	Conv (%)	Select A (%)
1	Dark	CH_3	O_2	27	0	0
2	Without catalyst	H	O_2	19	0	0
3	Without catalyst	CH_3	O_2	24	0	0
4	DPhCN-BTBT	CH_3	O_2	12	0	0
5	$CuSO_4$	CH_3	O_2	2	15.4	100
6	KI	CH_3	O_2	2	0	0
7	1,4-benzoquinone	CH_3	O_2	2	0	0
8	DABCO	CH_3	O_2	2	0	0
9	TEMPO	CH_3	O_2	2	0	0

[a] Photooxidation conditions: catalyst (2 mol%), sulfide (0.2 mmol), scavenger (0.2 mmol), acetonitrile (0.5 mL), irradiated by blue LED light (2x30W) at RT under O_2 balloon atmosphere.
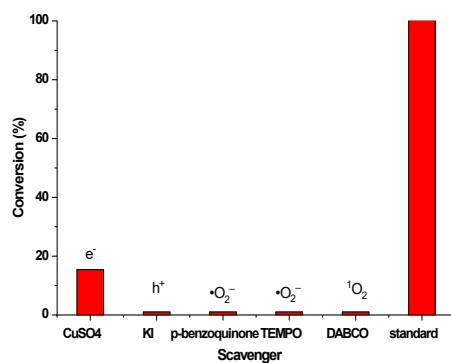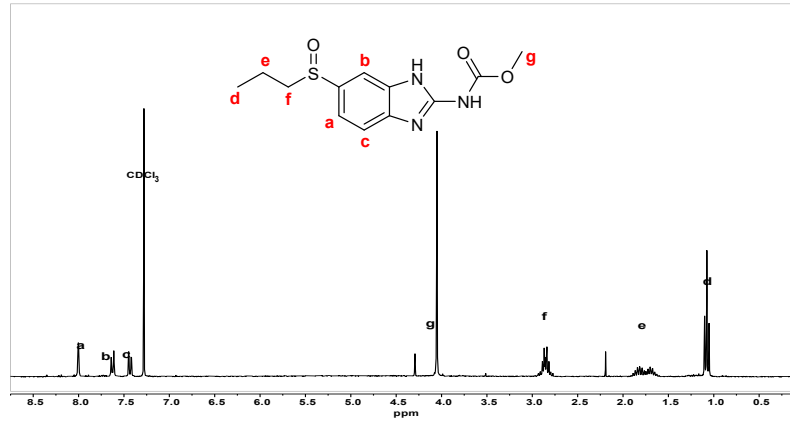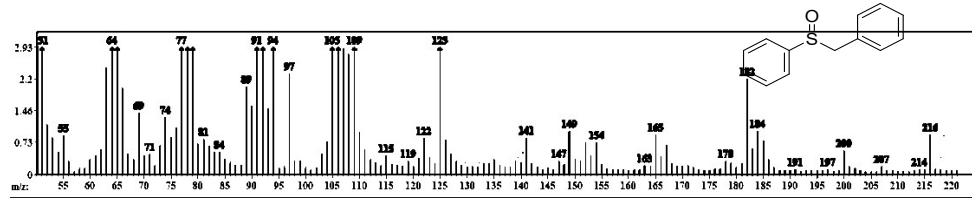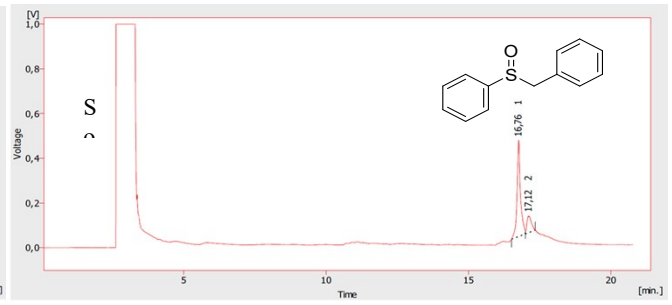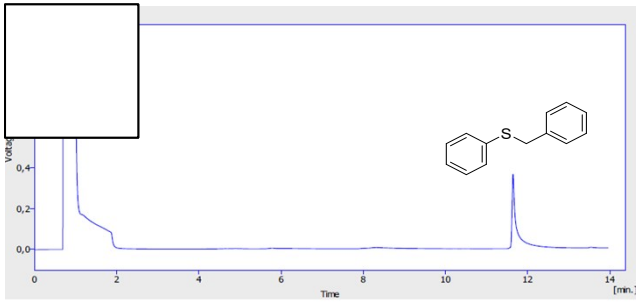
Figure S8. Control experiments in the presence of scavengers in the photosulfoxidation reaction. Representative GCs and NMR for the sulfoxidation reaction

Figure S9. Selected GC chromatograms, ^{1}H-NMR and HR-MS spectra of the photooxidation of sulfides
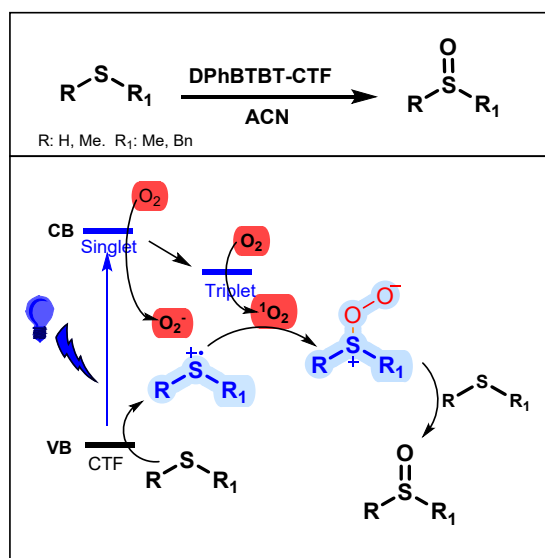
Cpd 1: C4 H9 Cl O S; 0.289: + FBF Spectrum (rt: 0.289 min)

141.0133
([C4H9ClOS]+H)+

Cpd 1: C12 H15 N3 O3 S; 2.049: + FBF Spectrum (rt: 2.032-2.066 min)

299.1182
([C12H15N3O3S]+NH4)+

Counts vs. Mass-to-Charge (m/z)
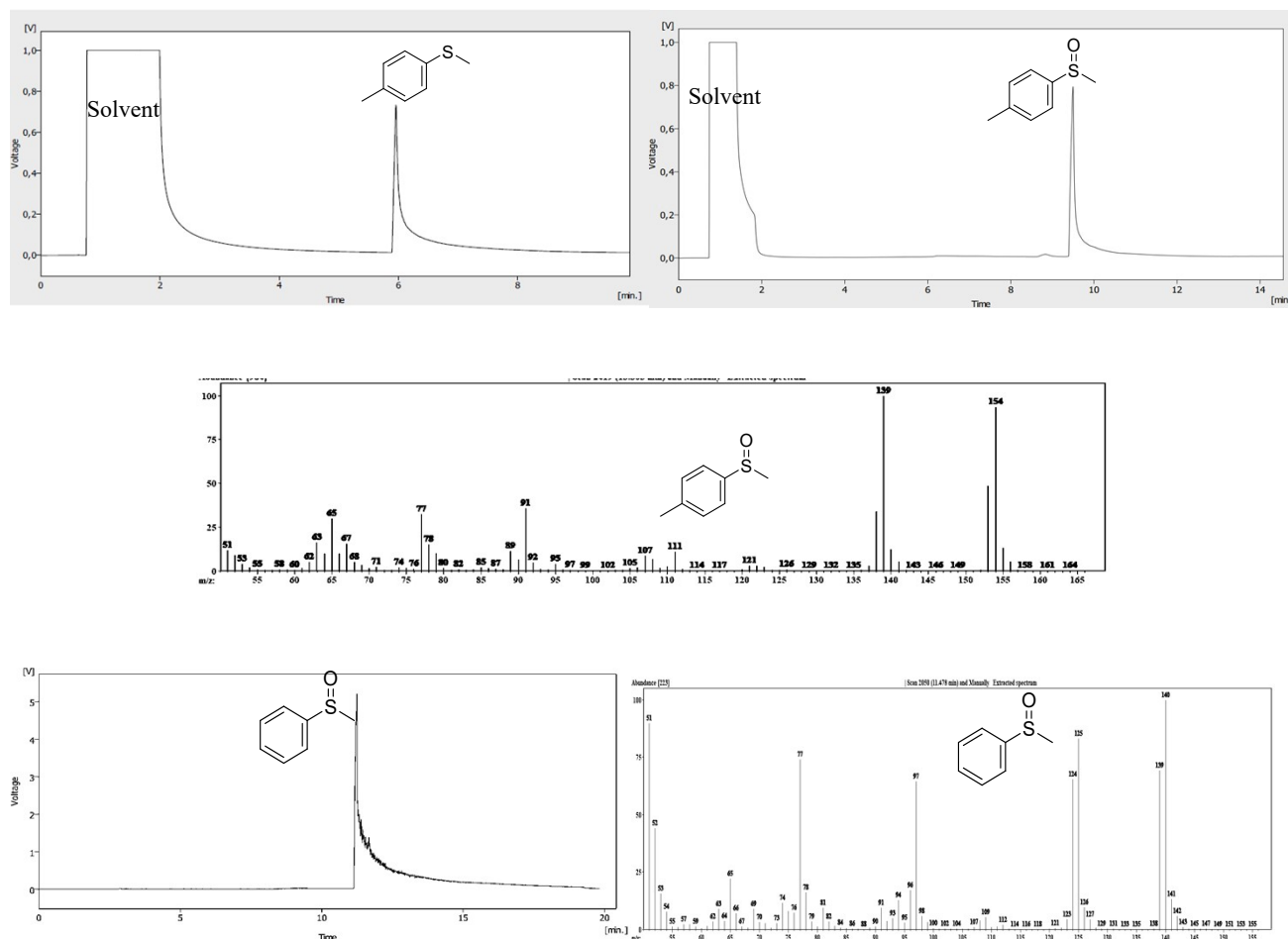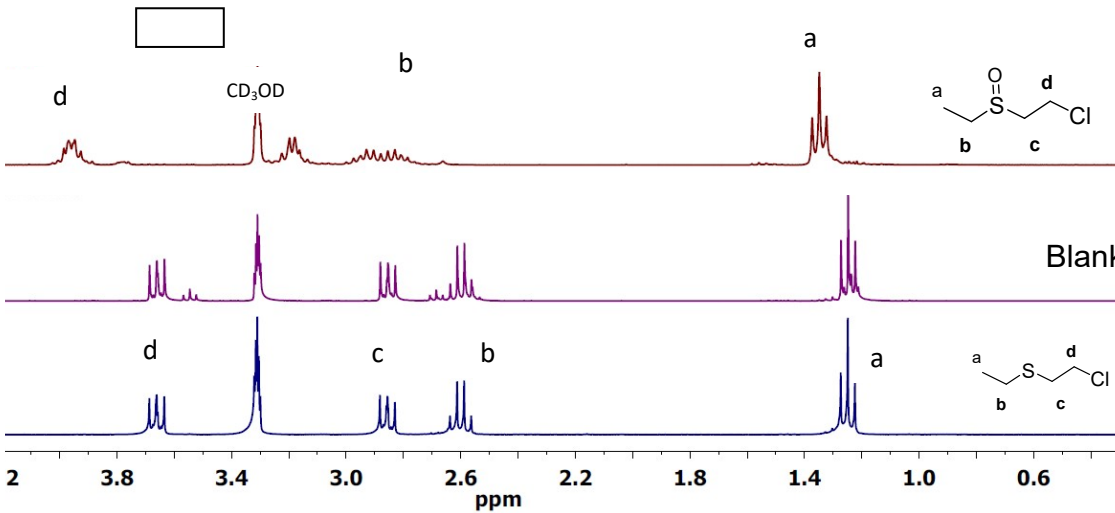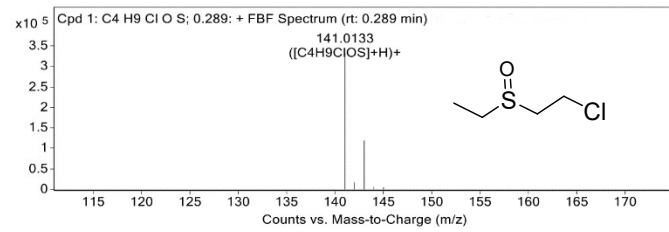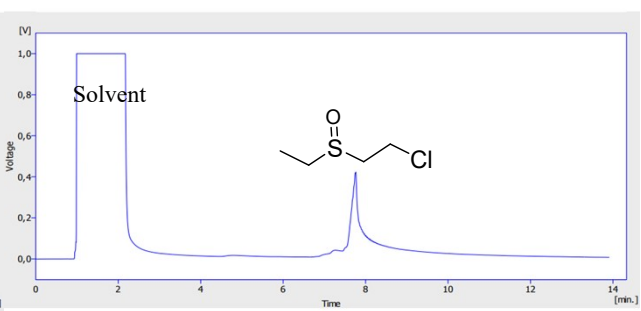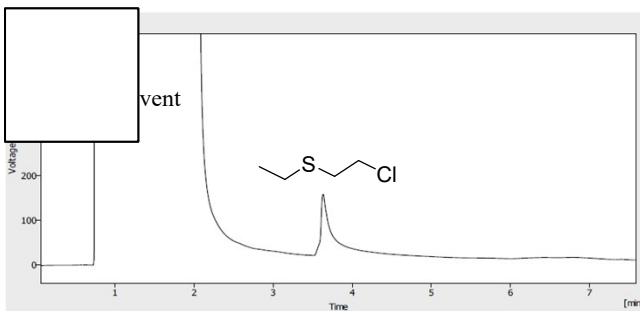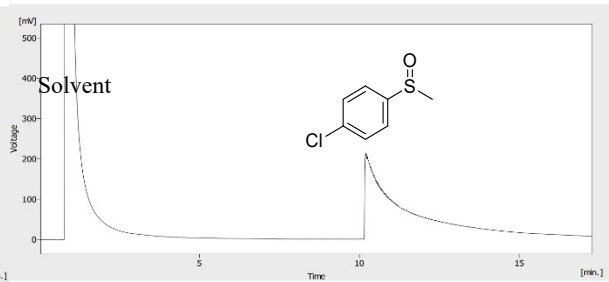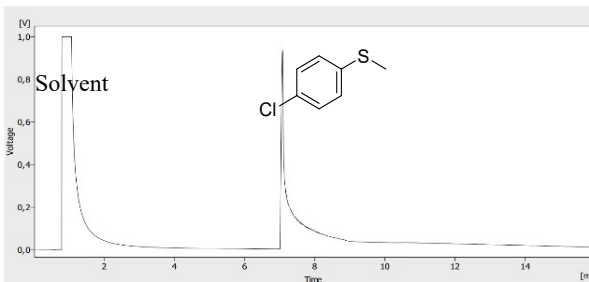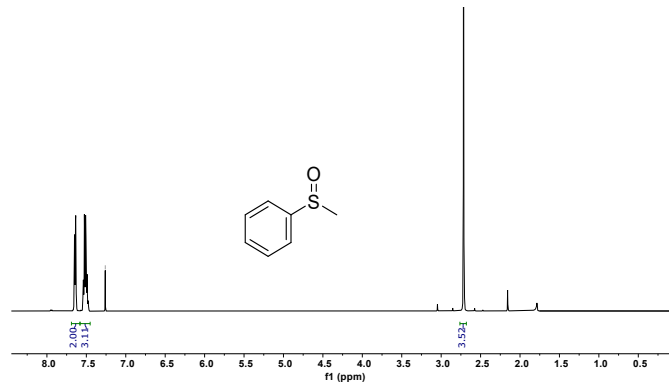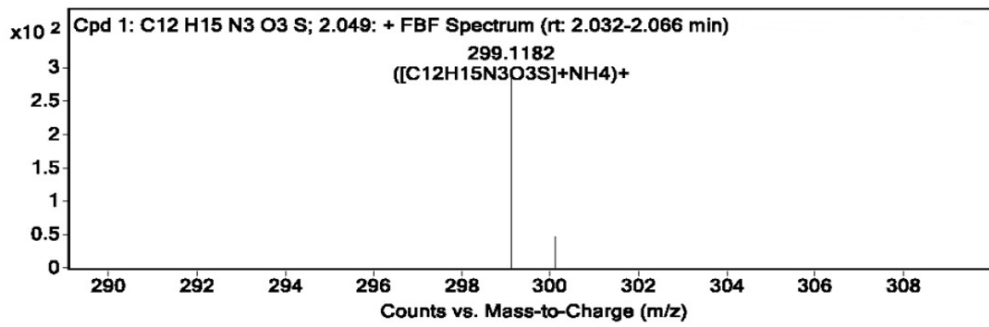
Figure S10. Mechanism proposed for photosulfoxidation.

5.2 Oxidation of Benzyl alcohols

General procedure: In a glass microreactor, the corresponding substrate (0.2 mmol), catalyst (2 mol%) and acetonitrile (0.5 mL) are added. The suspension was purged with O_2 and subjected to magnetic stirring and irradiation with blue LED light (2x30W) for the times indicated in table 2. The reactions were monitored by GC-MS chromatography.
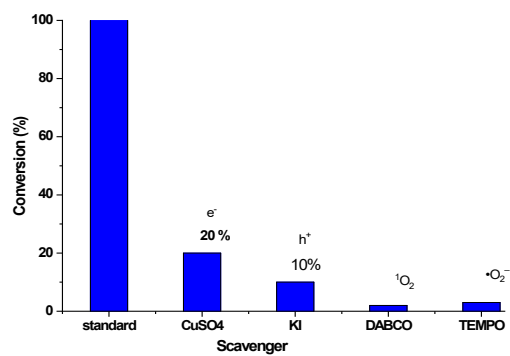
Figure S11. Selected GC chromatograms, ^{1}H-NMR and HR-MS spectra of the
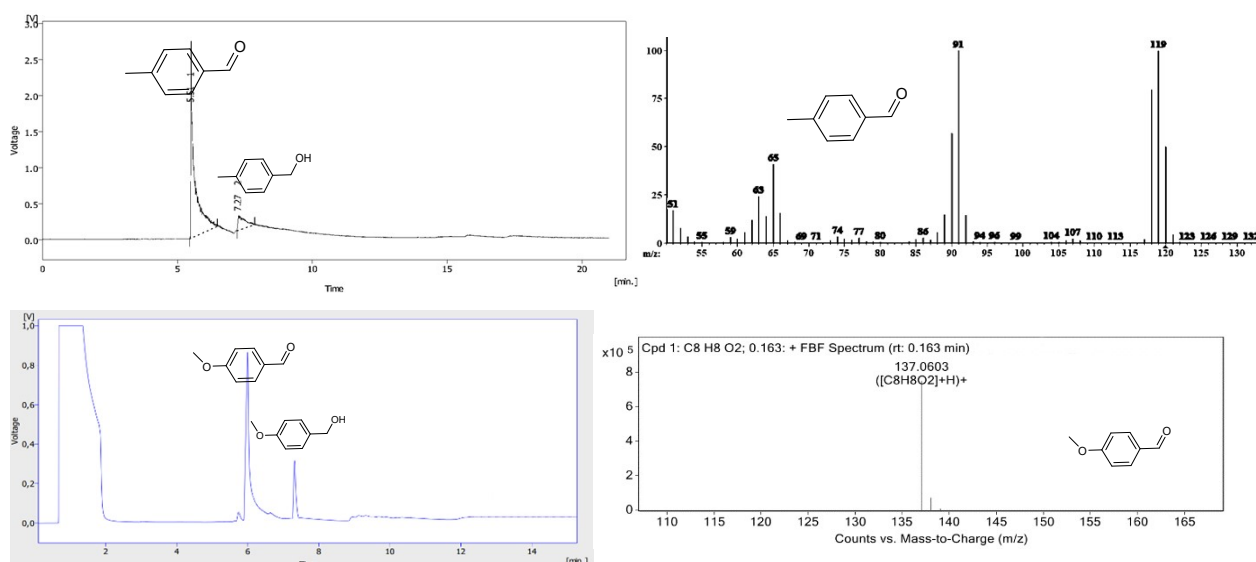
Figure S12. Control experiments in the presence of scavengers
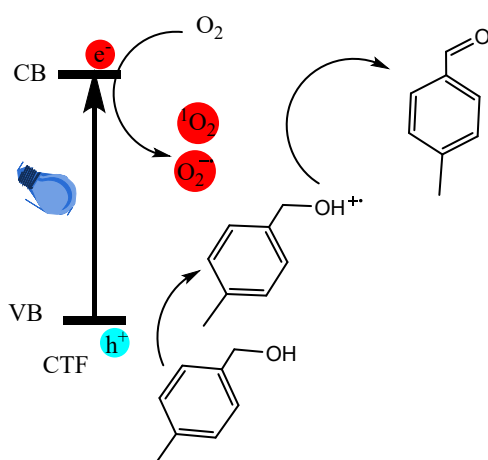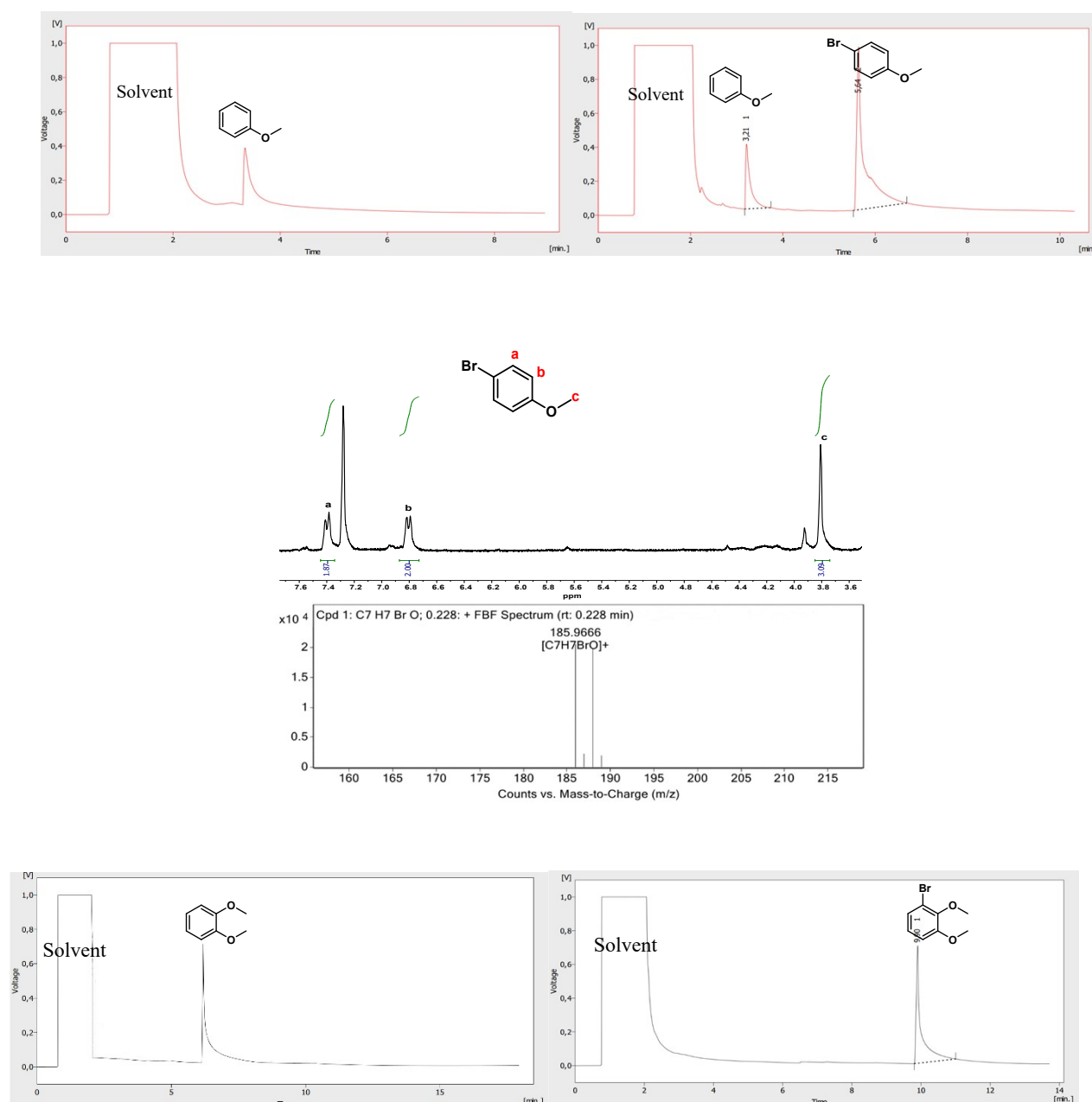

Figure S13. Proposed mechanism for benzyl alcohol oxidation.
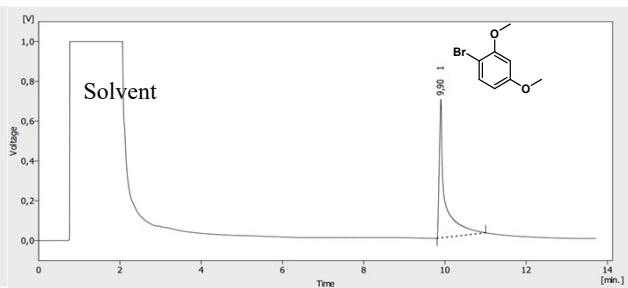
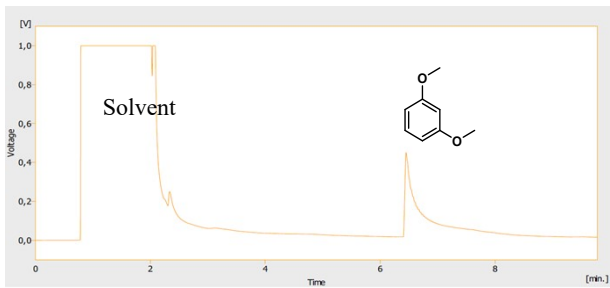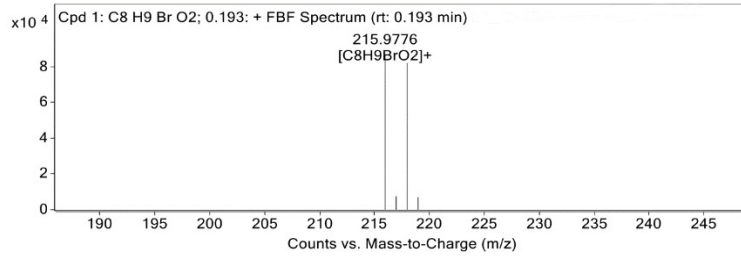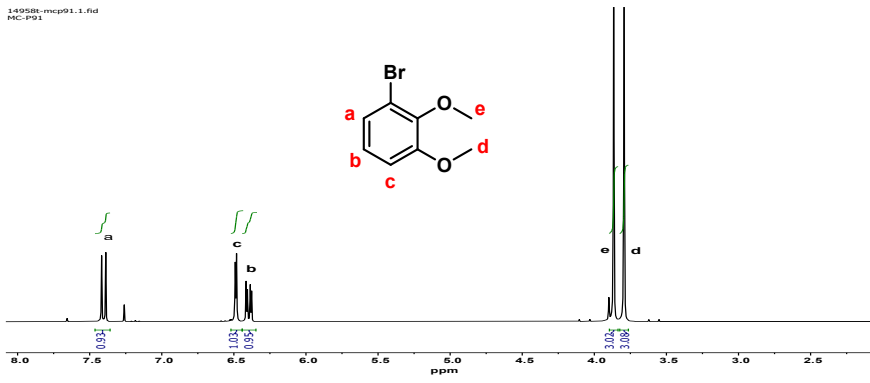## 5.3 Halogenation reactions

5.3.1 Bromination

General procedure: In a glass microreactor, the corresponding substrate (0.15 mmol), HBr 47% (1.05 mmol), catalyst (2 mol%) and acetonitrile (0.5 mL) are added. The suspension was purged with O_2 for 5 min and subjected to magnetic stirring and irradiation with blue LED light (2x30W). The reactions were monitored by GC chromatography and ^{1}H-NMR analysis.
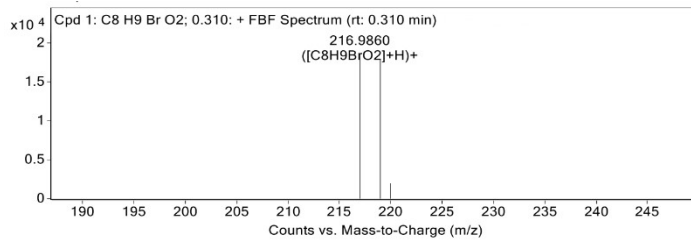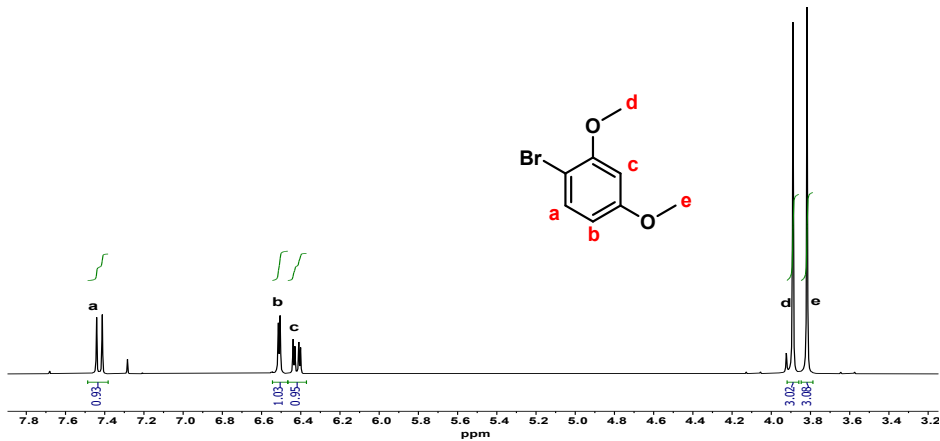
Figure S14. Selected GC chromatograms, ^{1}H-NMR and HR-MS spectra of the photocatalytic bromination of aromatic compounds

Cpd 1: C8 H9 Br O2; 0.193: + FBF Spectrum (rt: 0.193 min)
215.9776
[C8H9BrO2]+

Solvent

Solvent

Cpd 1: C8 H9 Br O2; 0.310: + FBF Spectrum (rt: 0.310 min)
216.9860
([C8H9BrO2]+H)+

14956t-mc85.1.fid
MC-85

Cpd 1: C9 H11 Br O3; 0.161: + FBF Spectrum (rt: 0.161 min)

246.9969
([C9H11BrO3]+H)+

Solvent

Solvent
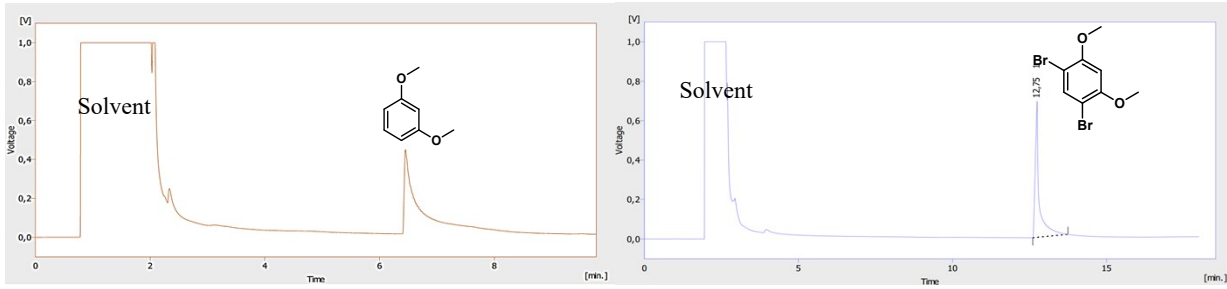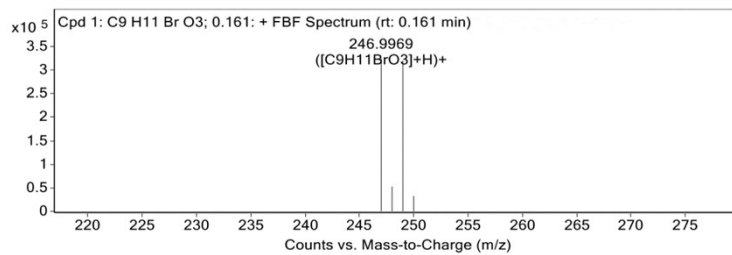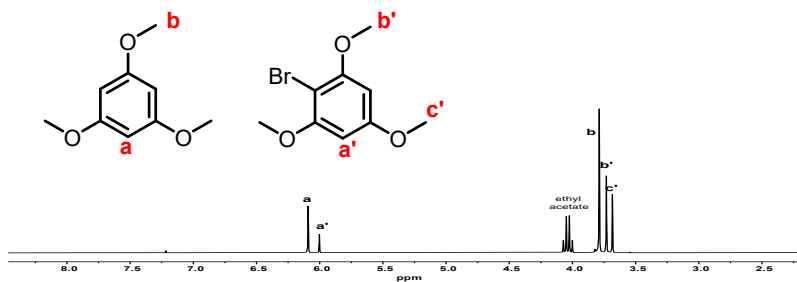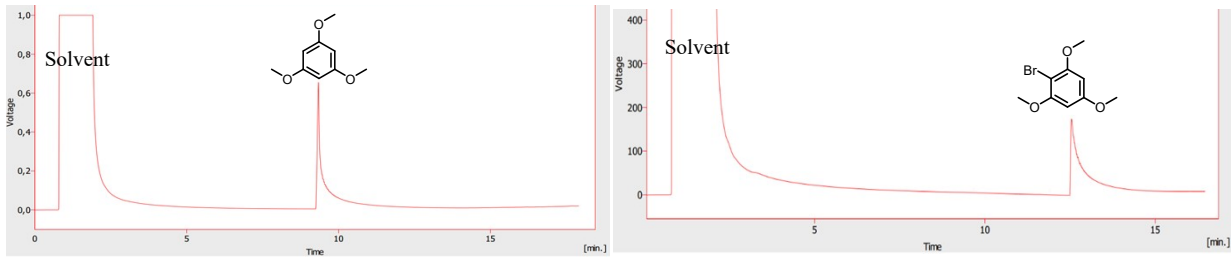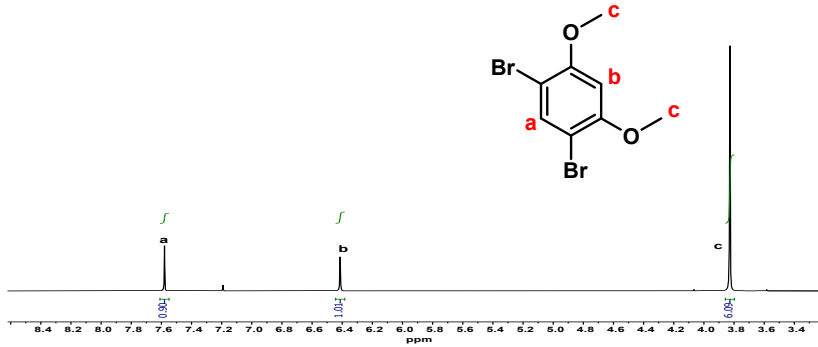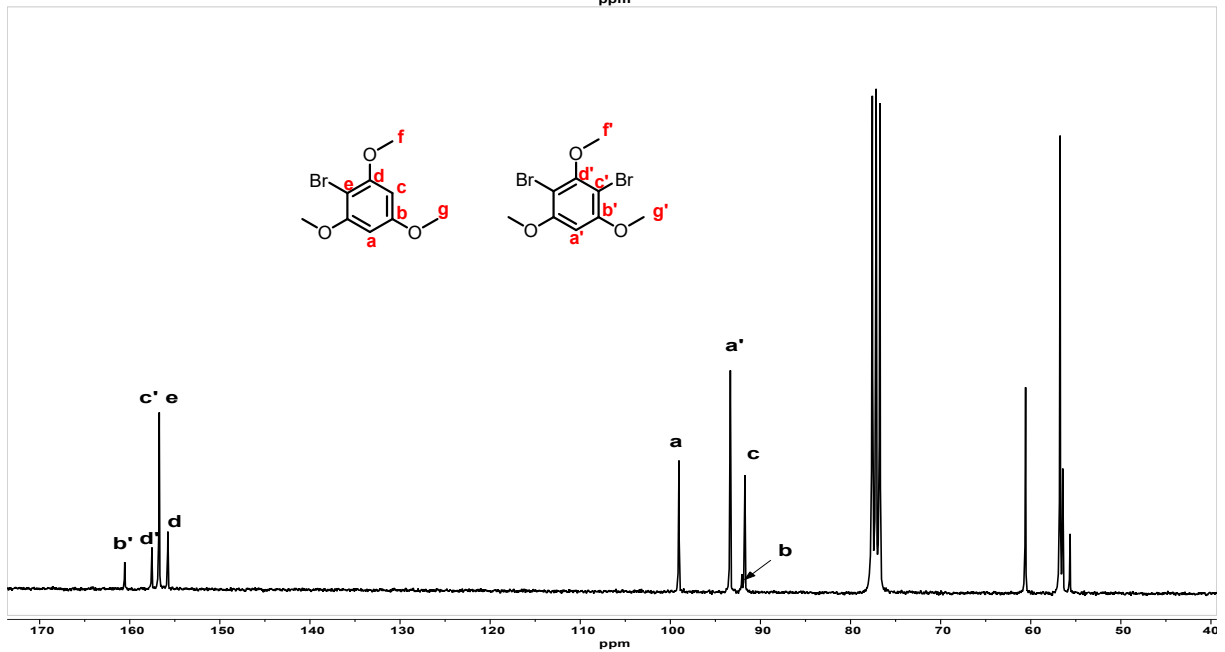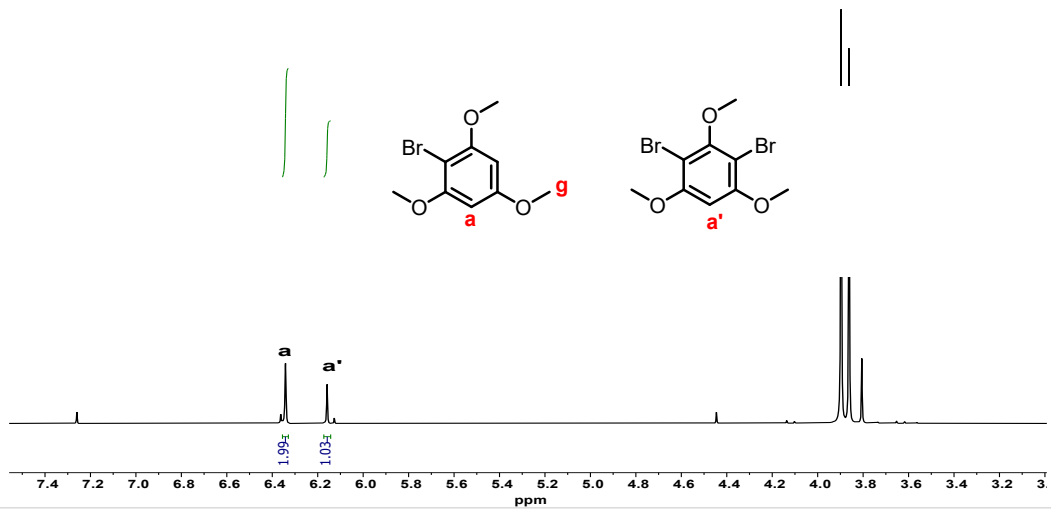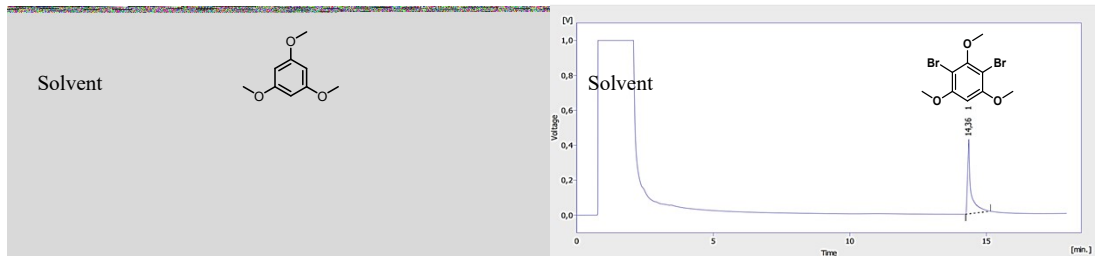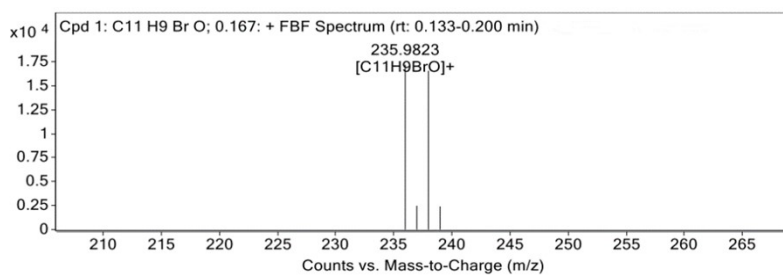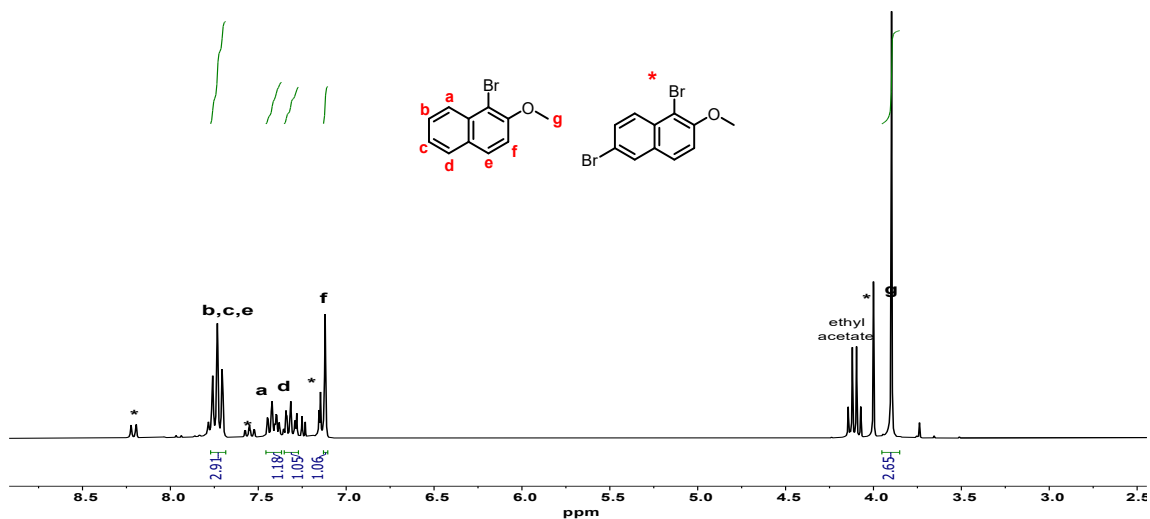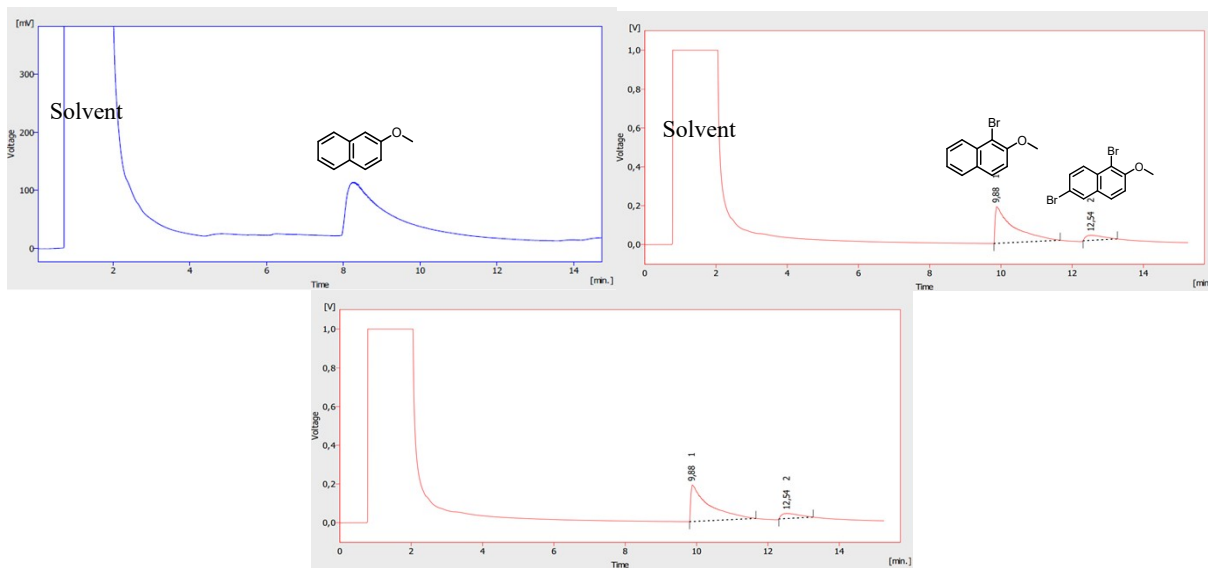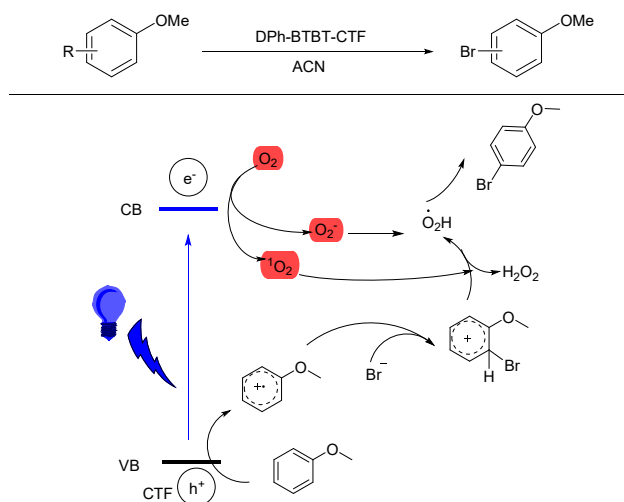
Figure S15. Proposed mechanism for the bromination reaction.

5.3.2 Chlorination

General procedure: In a glass microreactor, the corresponding substrate (0.15 mmol), HCl 37% (1.05 mmol), catalyst (2 mol%) and acetonitrile (0.5 mL) are added. The suspension was purged with O_2 for 5 min and subjected to magnetic stirring and irradiation with blue LED light (2x30W). The reactions were monitored by GC chromatography and ^{1}H-NMR analysis.

Figure S16. Selected GC chromatograms, ^{1}H-NMR and HR-MS spectra of the chlorination products

Cpd 1: C9 H11 Cl O3; 0.273: + FBF Spectrum (rt: 0.273-0.281 min)

203.0475
([C9H11ClO3]+H)+

Counts vs. Mass-to-Charge (m/z)

Solvent

Solvent

Cpd 1: C11 H9 Cl O; 0.259: + FBF Spectrum (rt: 0.262 min)

192.0324
[C11H9ClO]+

Counts vs. Mass-to-Charge (m/z)
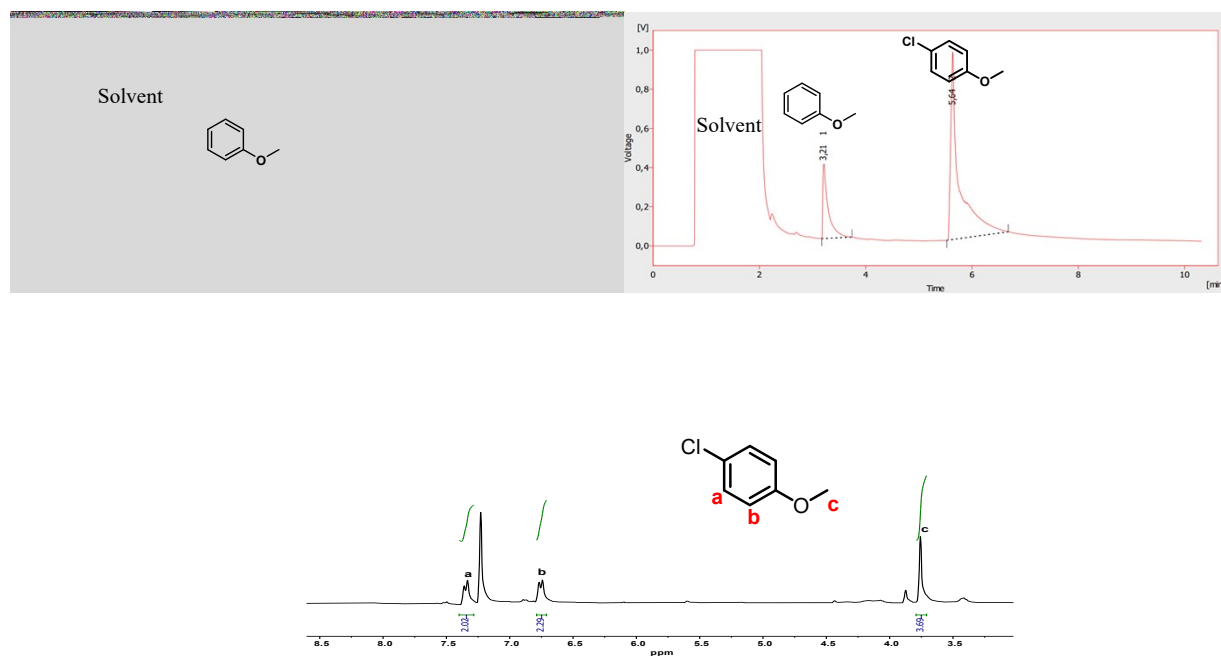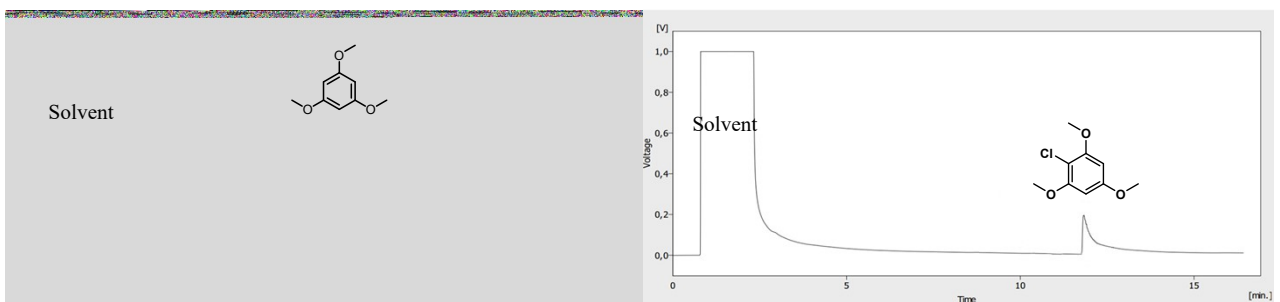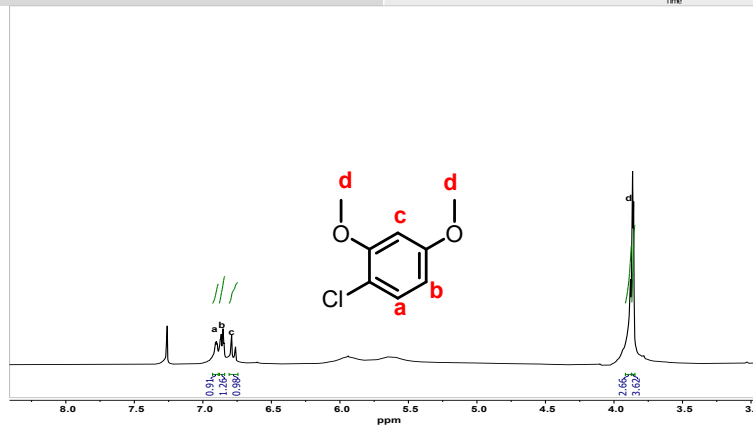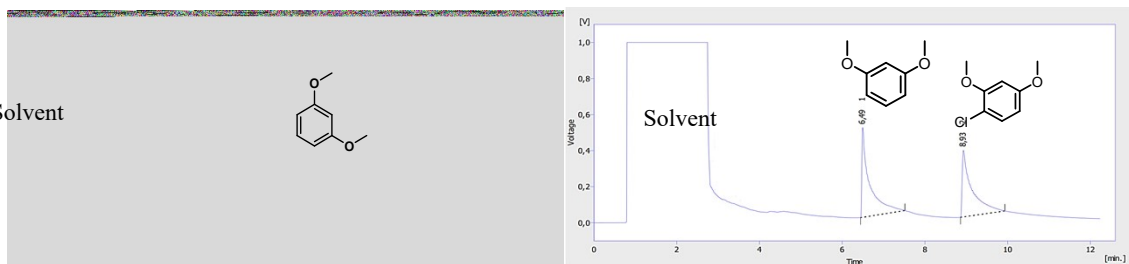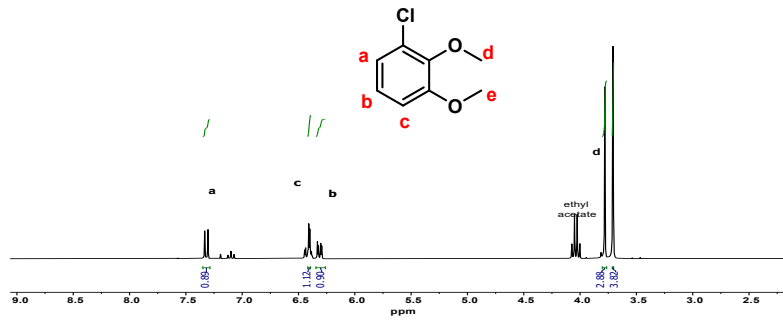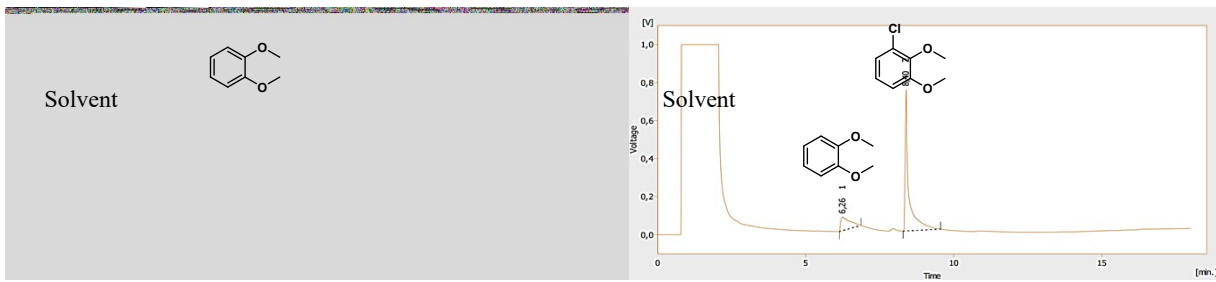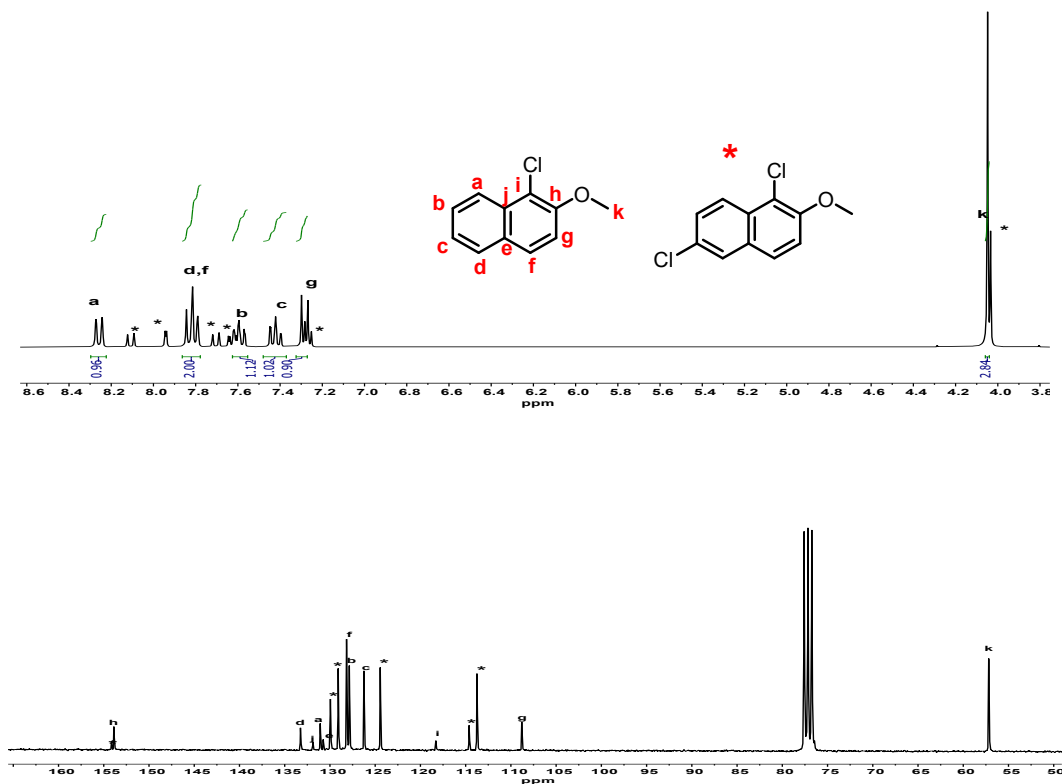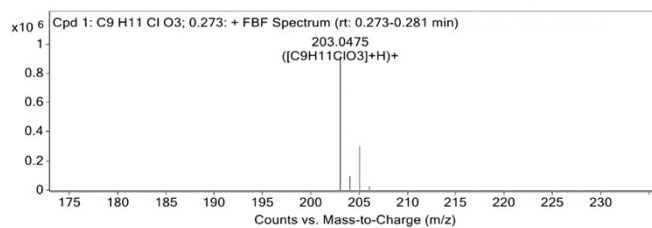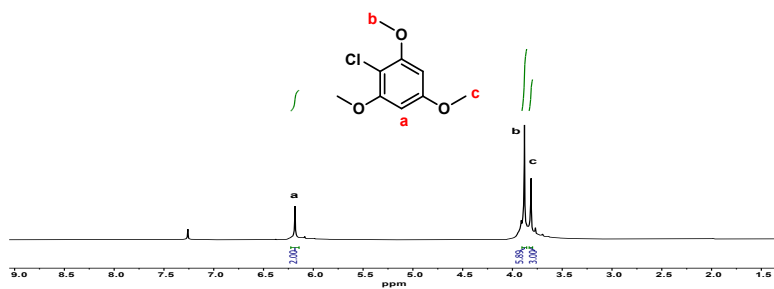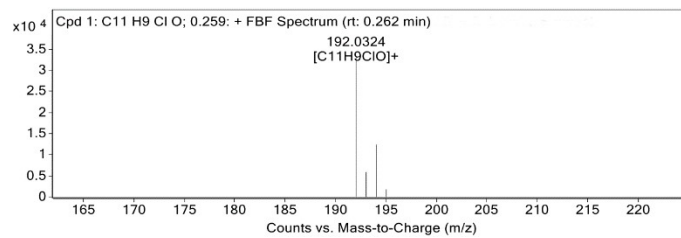
5.4 Other model reactions

5.4.1 Diels-Alder Cycloaddition

General procedure: In a glass microreactor, the corresponding diene (0.4 mmol – 3 eq), trans- anethole (0.13mmol – 1eq), catalyst (2 mol%) and acetonitrile (0.5 mL) are added. The suspension was purged with air and subjected to magnetic stirring and irradiation with blue LED light (2x30W) for 7 h. The reactions were monitored by GC and ^{1}H-NMR.

Quenching experiments were performed using both Diels-Alder substrates: 2,3-dimethyl-1,3-butadiene and trans-anethole. For the measurements, 1 mg of DPBTBT-CTF was mixed with the required amount of quencher in a total of 3 mL of dichloromethane in a 1x1 cm quartz cuvette. Solution of 0.25M of each substrate were prepared, the different added volumes of substrates solution, and corresponding final concentrations ([Q]), are shown **Table S3.**

Table S3. Volume added of 0.25M 2,3-dimethyl-1,3-butadiene and 0.25M trans-anethole solutions.

2,3-dimethyl-1,3-butadiene		trans-anethole	
Added volume (µL)	[Q] (mM)	Added volume(µL)	[Q] (mM)
0	0.0	0	0.0
10	0.84	10	0.84
10	1.68	10	1.68
10	2.52	10	2.52
10	3.35	10	3.35
10	4.17	20	5.00
10	5.00	40	8.20
10	5.80		
20	7.41		
20	9.00		
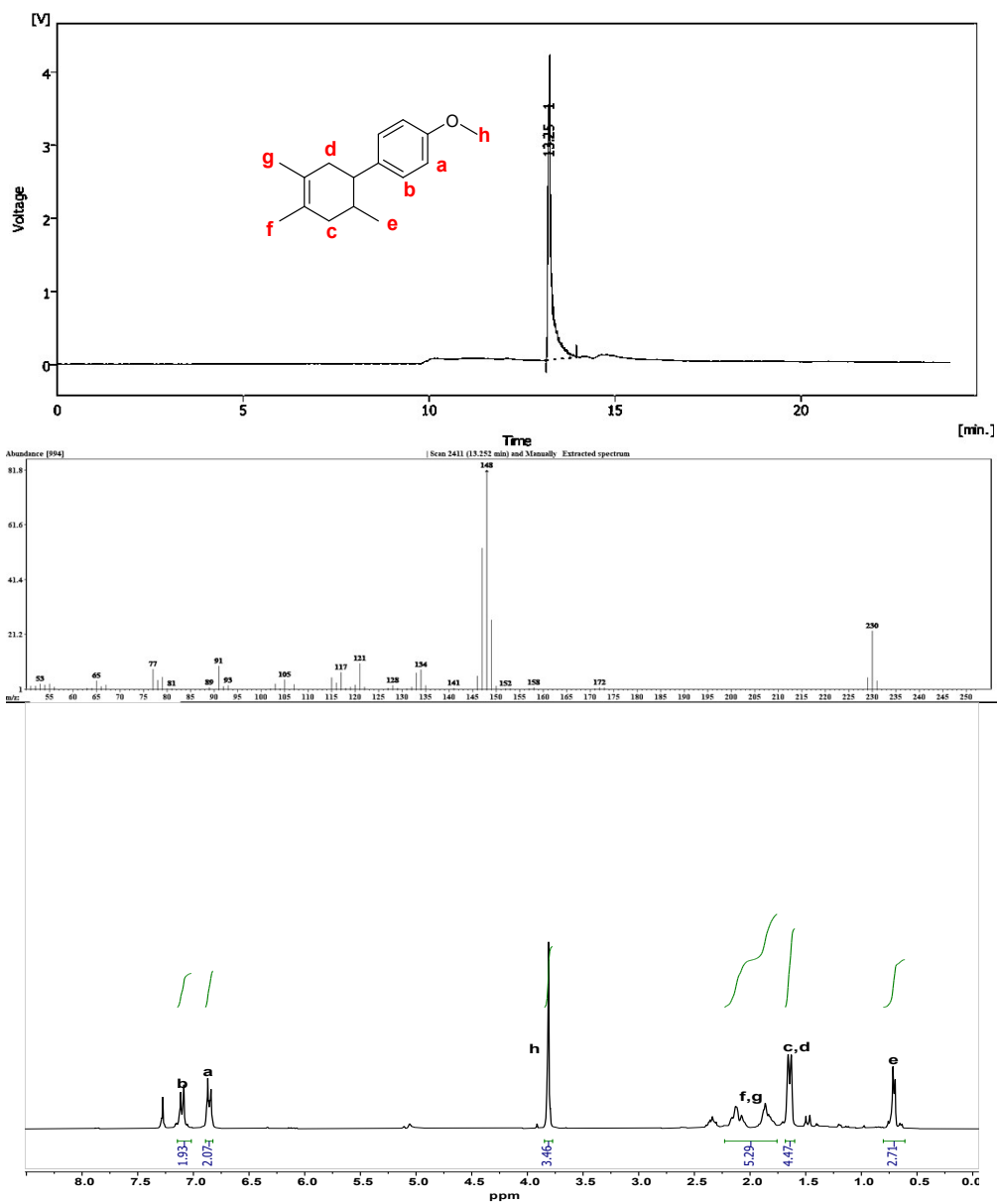
Figure S17.

5.4.2 Hydroxylation of phenylboronic acid

General procedure: In a glass microreactor, the corresponding substrate (0.2 mmol), trimethylamine (0.6mmol), catalyst (2 mol%) and tetrahydrofuran (0.5 mL) are added. The suspension was purged with O_2 and subjected to magnetic stirring and irradiation with blue LED light (2x30W) for 24 h. The reactions were monitored by ^{1}H-RMN.
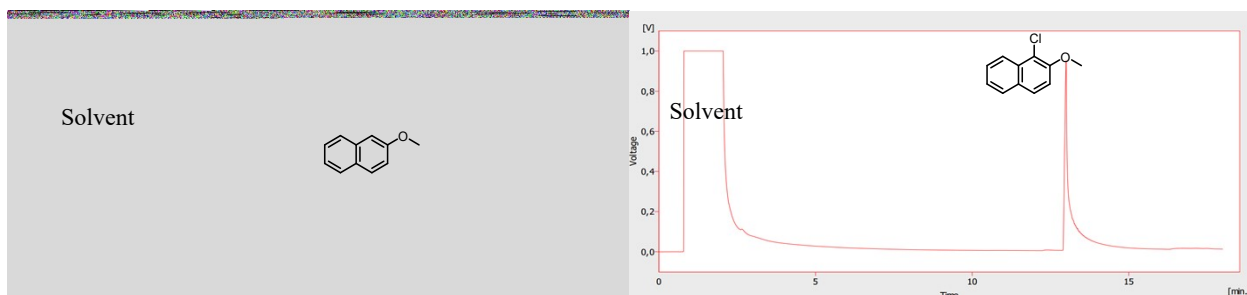

Figure S18.

6. Recycling experiments: Characterization of DPhBTBT-CTF after catalytic activity
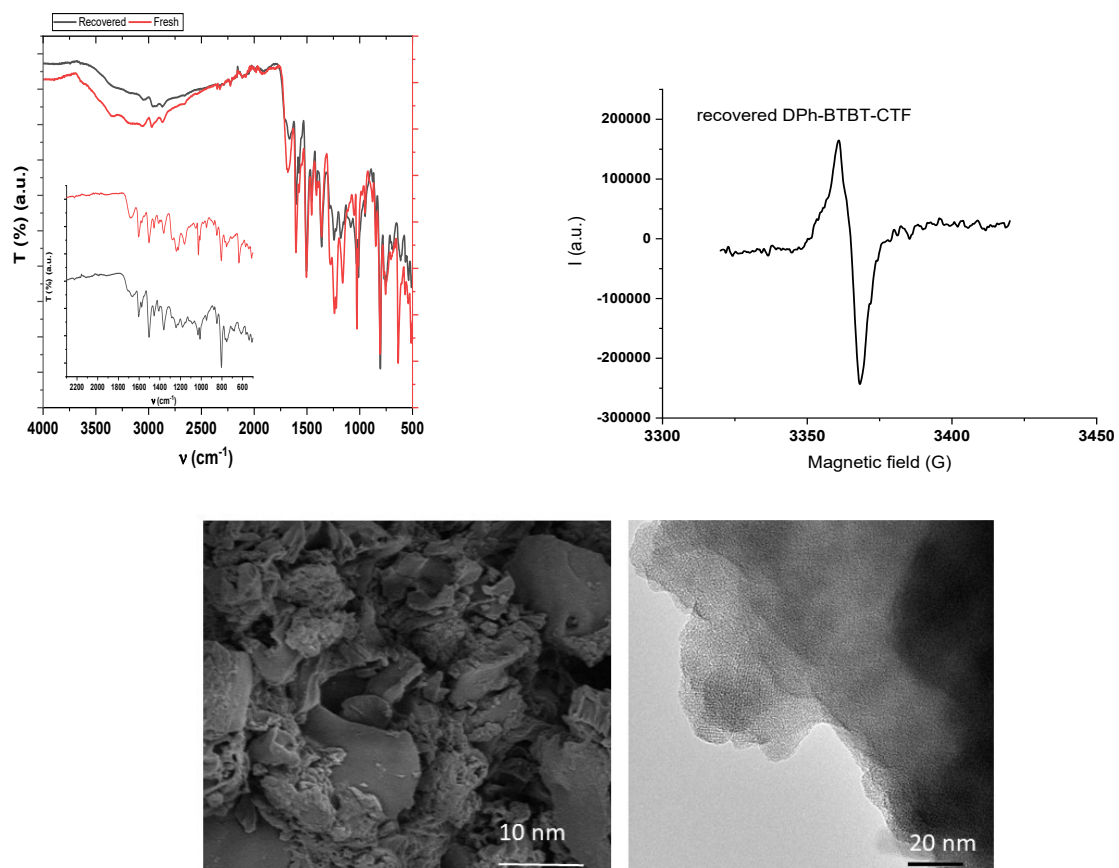
Figure S19. ATR-IR, EPR spectra, SEM and TEM images of recovered catalyst.

Table S4. Photosulfoxidation using different catalysts.

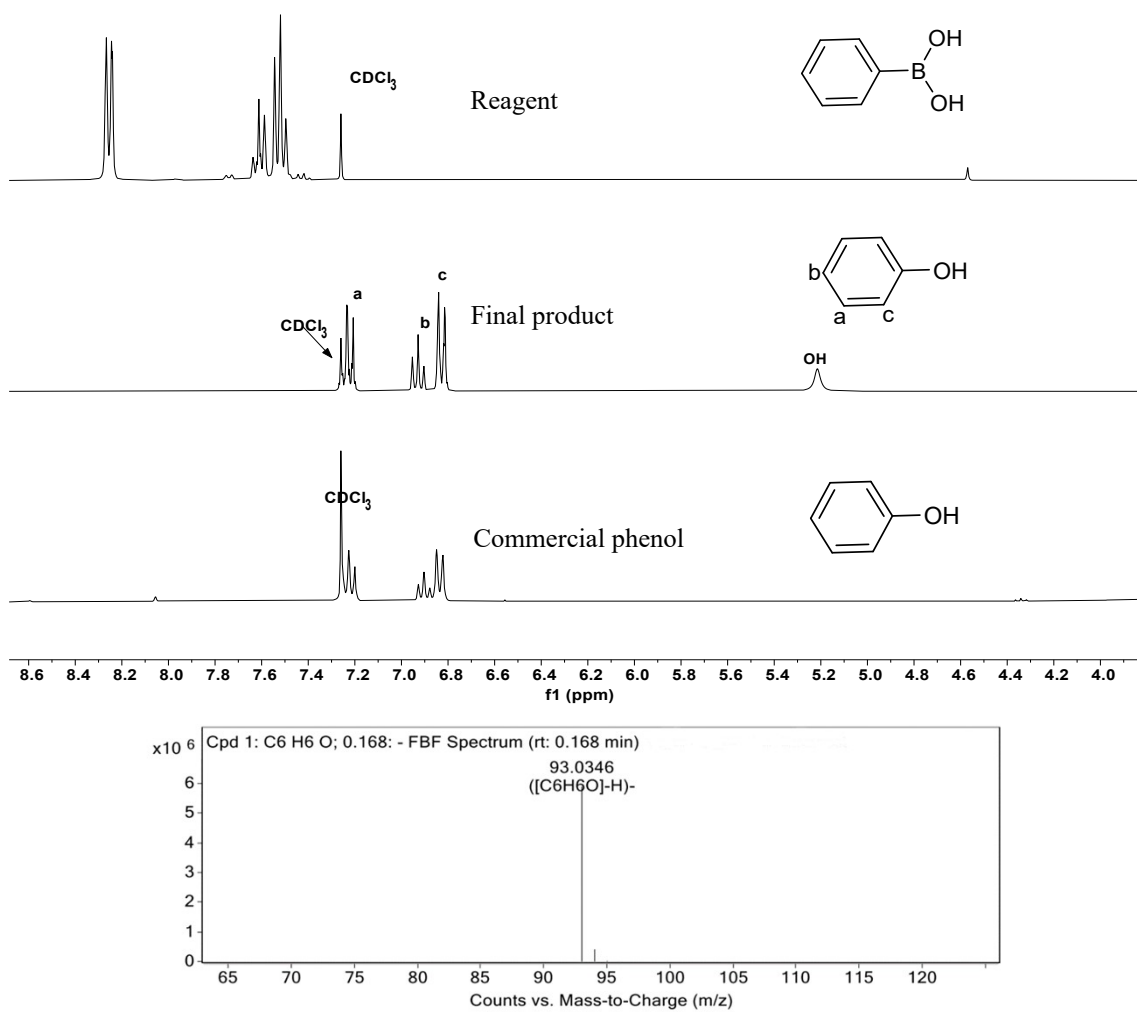| Entry	Photocatalyst	Conditions	t (h)	Conv. (%)	Sel. (%)
1	DPhBTBT-CTF (4.4 mg).[This work]	sulfide (0.2 mmol), MeCN (0.5 mL), blue LED light (2x30W) at RT, O_2 balloon, r.t.	5	>99	100
2	NDP-CTF (20 mg)[7]	sulfide (0.2 mmol), MeCN (0.5 mL), irradiated by blue LED light (50 W) at RT under O_2/air, r.t.	1	100	100
3	TCPP-CMP (10 mg)[8]	sulfide (0.5 mmol), CH_3CN /H_2O (10 mL, 1 : 1 v/v), O_2 (1 atm), white LED (100 W), 25 °C.	16	99	97
4	TzTz-TA (4 mg)[9]	sulfide (0.3 mmol), CH_3OH (1 mL), blue LEDs (460 ± 10 nm), air (1 atm)	0.3	93	99
5	NQ-COFTfppyPh (5 mg)[10]	sulfide (0.1 mmol), CH_3OH (1.5 mL), O_2, LED lamp (18 W, 460-465 nm), r.t.	12	99	--
6	TTT-COF (4 mg)[11]	sulfide (0.3 mmol), C_2H_5OH (1 mL), O_2 (1 atm), blue LEDs irradiation (460 ± 10 nm), r.t.]	0.5	99	99
7	Pt@COF (2.4 mg)[12]	sulfide (0.3 mmol), CH_3OH (2.0 mL), O_2 atmosphere, LED (λ = 450 nm), 25 °C.	12	96	–
8	Degussa P25 TiO_2 (40 mg)[13]	sulfide (0.3 mmol), TEA (0.03 mmol), CH_3OH (5 mL), O_2 (1atm), Xe lamp (300 W, λ >420 nm), r.t.	10	84	92
9	AQ-COF (10 mg)[14]	sulfide (0.1 mmol), CH_3CN (2 mL), O_2 (1 atm), Xe lamp (300 W, λ = 400–780 nm), r.t.	3.0	>99	97
10	$Bi_4O_5Br_2$ (20 mg)[15]	sulfide (0.2 mmol), H_2O (1 mL), O_2 (1 atm), a blue LED (30 W, Kessil PR160-456 nm).	6	99	98
11	BODIPY (2.5μmol)[16]	sulfide (0.5 mmol), CH_3OH (0.5 mL), air (1 atm), fluorescent lamp (24W, λ = 395 nm), r.t.	24	89	--
12	B-(Boc-CB)2-BT (10 mg)[17]	flow rate of sulfides in CH_3CN: 1 mL min−1, air (1 atm), LED (4.5 W, λ = 460 nm), r.t.	24	99	95
13[18]	spherical-COF1a	Blue LED		100	
	laminar-COF1b			100	
	3D-COF1c			99	
14	A_2B_2-Pro-COF[19]	Xenon lamp		96	
15	h-LZU1[20]	Xenon lamp		100	
17	Sn-CPF3[21]	Blue LED		99	

Table S5. Photohalogenation using different catalysts.

Entry	Photocatalyst	Substrate	Conditions	t (h)	Conv. (%)	Sel. (%)
1	DPhBTBT-CTF (4.4 mg). This work	anisole	substrate (0.15 mmol), HBr 47% (1.05 mmol) or HCl 37% (1.05 mmol), MeCN (0.5 mL), blue LED light (2x30W), r.t.	1.15/13	100	1-Br/1-Cl
2		1,3,5-trimethoxybenzene		0.5	75	1-Br
3				6/4	100	34:66 (2-Br: 2,4-Br)/2-Cl
4		1,3-dimethoxybenzene		1.15	100	1-Br
5				6/20	100	1,5-Br/1-Cl
7	PYT (4 mg)[22]	anisole	substrate (0.6 mmol); HBr (0.6 mL, 48 wt.%); MeCN (3 mL), 461 nm	48	97	1-Br
8		1,3,5-trimethoxybenzene		24	81	1:1 (2-Br: 2,4-Br)
8		1,3-dimethoxybenzene		49	95	2,4-Br
9	K-PHI (4 mg)[23]	anisole	substrate 0.02 mmol; HCl (36 wt. %) 0.1 mL; MeCN 0.5 mL; T = 30 °C; 465 nm	24	100	1-Br
10		1,3,5-trimethoxybenzene		24	100	2,4-Br
11		1,3-dimethoxybenzene		24	100	1-Br
12		anisole		24	100	1:0.31 (1-Cl:2-Cl)
13		1,3,5-trimethoxybenzene		24	100	1:0.31 (1-Cl: 2,4-Cl)

7. References

[1] M. Saito, I. Osaka, E. Miyazaki, K. Takimiya, H. Kuwabara and M. Ikeda, *Tetrahedron Lett.*, 2011, **52**, 285–288. https://doi.org/10.1016/j.tetlet.2010.11.021

[2] H. Monobe, L. An, P. Hu, B. Q. Wang, K. Q. Zhao and Y. Shimizu, *Mol. Cryst. Liq.,* 2017, **647**, 119–126. https://doi.org/10.1080/15421406.2017.1289443.

[3] A. Sanzone, S. Mattiello, G. M. Garavaglia, A. M. Calascibetta, C. Ceriani, M. Sassi and L. Beverina, *Green Chem.*, 2019, **21**, 4400–4405. https://doi.org/10.1039/c9gc01071h.

[4] C. Yao, X. Chen, Y. He, Y. Guo, I. Murtaza, H. Meng, *RSC Adv.*, 2017, **7**, 5514–5518. https://doi.org/10.1039/c6ra28074a

[5] Y. He, S. Guo, Y. He, I. Murtaza, A. Li, X. Zeng, Y. Guo, Y. Zhao, X. Chen and H. Meng. *Chem. Eur. J.* 2018, **24**, 16595 – 16602. https://doi.org/10.1002/chem.201803542

[6] K. Takimiya, H. Ebata, K. Sakamoto, T. Izawa, T. Otsubo, Y. Kunugi, *J. Am. Chem. Soc.*, 2006, **128**, 12604–12605. https://doi.org/10.1021/ja064052l

[7] B. Fuerte-Díez, A. Valverde-González, M. Pintado-Sierra, U. Díaz, F.Sánchez, E. M. Maya, M. Iglesias *Solar RRL*, 2022, **6**, 1–10. https://doi.org/10.1002/solr.202100848

[8] J. Jiang, Z.X. Liang, X.Y. Xiong, X.T. Zhou, H.B. Ji, *ChemCatChem*, 2020, *12*, 3523-3529, https://doi.org/10.1002/cctc.202000199.

[9] Y. Wang, X. Li, X. Dong, F. Zhang, X.Lang, *J. Colloid Interface Sci.*, 2022, **616**, 846-857, https://doi.org/10.1016/j.jcis.2022.02.114.

[10] X.D. Zhao, H.J. Pang, D.K. Huang, G. Liu, J.X. Hu, Y.G. Xiang, *Angew. Chem. Int. Ed.*, 2022, **61**, e202208833, https://doi.org/10.1002/anie.202208833.

[11] Y. Wang, F. Huang, W. Sheng, X. Miao, X. Li, X.-K. Gu, X. Lang, *Appl. Catal. B: Environ.* 2023, **338**, 123070. https://doi.org/10.1016/j.apcatb.2023.123070

[12] A. Lopez-Magano, A.E. Platero-Prats, S. Cabrera, R. Mas-Balleste, J. Aleman, *Appl. Catal. B: Environ* 2020, **272**, 119027, https://doi.org/10.1016/j.apcatb.2020.119027.

[13] X.J. Lang, W. Hao, W.R. Leow, S.Z. Li, J.C. Zhao, X.D. Chen, *Chem. Sci.*, 2015, **6**, 5000–5005, https://doi.org/10.1039/c5sc01813g.

[14] Q. Li, X.W. Lan, G.Y. An, L. Ricardez-Sandoval, Z.G. Wang, G.Y. Bai, *ACS Catal.*, 2020, **10**, 6664–6675, https://doi.org/10.1021/acscatal.0c00290.

[15] W. Zhao, C.X. Yang, J.D. Huang, X.L. Jin, Y. Deng, L. Wang, F.Y. Su, H.Q. Xie, P.K. Wong, L.Q. Ye, *Green Chem.*, 2020, **22**, 4884–4889, https://doi.org/10.1039/d0gc01930e.

[16] W.L. Li, Z.G. Xie, X.B. Jing, *Catal. Commun.*, 2011, **16**, 94–97, https://doi.org/10.1016/j.catcom.2011.09.007.

[17] Z.J. Wang, S. Ghasimi, K. Landfester, K.A.I. Zhang, *Chem. Commun.*, 2014, **50**, 8177–8180, https://doi.org/10.1039/c4cc02861a.

[18] H. Chen, H. S. Jena, X. Feng, K. Leus and P. Van Der Voort, *Angew. Chem. – Int. Ed.,* 2022, **61**, e20220493. DOI:10.1002/anie.202204938.

[19] W. Hao, D. Chen, Y. Li, Z. Yang, G. Xing, J. Li, L. Chen, *Chem. Mater.* 2019, **31**, 8100–8105. https://doi.org/10.1021/acs.chemmater.9b02718

[20] L. Liu, B. Zhang, X. Tan, D. Tan, X. Cheng, B. Han, J. Zhang, *Chem. Commun*. 2020, **56**, 4567–4570. DOI: 10.1039/D0CC00761G

[21] X. Wang, M.-J. Dong, C.-D. Wu, *Nanoscale* 2020, **12**, 16136– 16142. DOI: 10.1039/D0NR02994G

[22] Y. Zou, S. Abednatanzi, P. Gohari Derakhshandeh, S. Mazzanti, C. M. Schüßlbauer, D. Cruz, P. Van Der Voort, J.-Wen Shi, M.Antonietti, D. M. Guldi, A. Savateev *Nat. Commun.* 2022, **13**, 2171. https://doi.org/10.1038/s41467-022-29781-9

[23] Y. Markushyna, C. Teutloff, B. Kurpil, D. Cruz, I. Lauermann, Y. Zhao, M. Antonietti and A. Savateev, *Appl. Catal. B: Environ* 2019, **248**, 211–217. https://doi.org/10.1016/j.apcatb.2019.02.016